Supplementary Case Report for a Generalized Linear Model Lecture

Sridevi Sarma, PhD

Department of Applied Mathematics and Statistics
Boston University
Boston, Massachusetts

Institute for Computational Medicine
Department of Biomedical Engineering
Johns Hopkins University
Baltimore, Maryland

Introduction: Spiking Patterns in Parkinson's Disease and in Health

The placement of deep-brain stimulating electrodes in the subthalamic nucleus (STN) to treat Parkinson's disease (PD) also allows the recording of single neuron spiking activity. Analyses of these unique data offer an important opportunity to better understand the pathophysiology of PD. However, despite the point-process nature of PD neural spiking activity, point-process methods are rarely used to analyze these recordings.

We developed a point-process representation of PD neural spiking activity using a generalized linear model (GLM) to describe long- and short-term temporal dependencies in the spiking activity of 28 STN neurons from seven PD patients, and 35 neurons from one healthy primate (surrogate control), recorded while the subjects executed a directed hand-movement task. We used the point-process model to characterize each neuron's bursting, oscillatory, and directional tuning properties during key periods in the task trial. Relative to the control neurons, the PD neurons showed increased bursting, increased 10–30 Hz oscillations, and increased fluctuations in directional tuning. These features, which traditional methods failed to capture accurately, were efficiently summarized in a single model in the point-process analysis of each neuron. The point-process framework suggests a useful approach for developing quantitative neural correlates that may be related directly to the movement and behavioral disorders characteristic of PD.

The GLM lecture described how one can model neural responses to stimuli with a generalized notion of linear regression. This supplementary document shows a published case study (Sarma et al., 2010) on how GLMs can be used to both model neuronal spiking data in response to a motor behavioral stimulus and make inferences about spiking patterns from model parameters.

Behavioral task

Once microelectrodes were placed in the STN, the subjects viewed a computer monitor and performed a behavioral task by moving a joystick with the contralateral hand. The joystick was mounted such that movements were in a horizontal orientation with the elbow flexed at approximately 45°. The behavioral task began with the presentation of a small central fixation point. After a 500 ms delay, four small gray targets appeared arrayed in a circular fashion around the fixation point (up, right, down, and left). After a 500–1,000 ms delay, a randomly selected target turned green (target cue [TC]) to indicate where the subject was to move. Then, after another 500–1,000 ms delay, the central fixation point turned green (go cue [GC]), cueing the subject to move. At this point, the subject used the joystick to guide a cursor from the center of the monitor toward the green target. Once the target was reached, either a juice reward was given (in the primate case) or a tone sounded, indicating that the subject had successfully completed the task (human case) and the stimuli were erased. Subjects were required to return the joystick to the center position before the next trial started. A schematic representation of a single trial is shown in Figure 1.

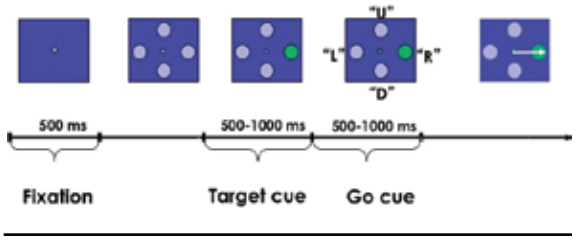

Figure 1. Schematic of a behavioral task trial. U, R, D, L = Up, Right, Down, Left.

Point-process model of STN dynamics

We formulated a point-process model to relate the spiking propensity of each STN neuron to factors associated with movement direction and features of the neuron's spiking history. We used the model parameters to analyze oscillations, bursting, and directional tuning modulations across the entire trial and to make comparisons between two subject groups. A point process is a series of 01 random events that occur in continuous time. For a neural spike train, the 1s are individual spike times and the 0s are the times at which no spikes occur. To define a point-process model of neural spiking activity, in this analysis we considered an observation interval $(0, T]$ and let $N(t)$ be the number of spikes counted in interval $(0, t]$ for $t \in (0, T]$. A point-process model of a neural spike train can be completely characterized by its cumulative intensity function (CIF), $\lambda(t|Ht)$, defined as follows:

$$\lambda(t|H_t) = \lim_{\Delta \to 0} Pr(N(t+\Delta) - N(t) = 1 | H_t)/\Delta \quad (1)$$

where H_t denotes the history of spikes up to time t. It follows from equation (2) that the probability of a single spike in a small interval $(t, t + \Delta]$ is approximately

$$Pr(\text{spike in } (t, t + \Delta] \mid H_t) = \lambda(t|H_t)\,\Delta \quad (2)$$

NOTES

(Details can be found in Snyder and Miller, 1991, and Cox and Isham, 2000.) When Δ is small, equation (2) approximates the spiking propensity at time t.

The CIF generalizes the rate function of a Poisson process to a rate function that is history dependent. Because the conditional intensity function completely characterizes a spike train, defining a model for the CIF defines a model for the spike train (Brown et al., 2003; Brown, 2005). For our analyses, we used the GLM to define our CIF models by expressing, for each neuron, the log of its CIF in terms of the neuron's spike history and relevant movement covariates (Truccollo et al., 2005). The GLM is an extension of the multiple linear regression model in which the variable being predicted (in this case, spike times) need not be Gaussian (McCullagh and Nelder, 1989). GLM also provides an efficient computational scheme for estimating model parameters and a likelihood framework for conducting statistical inferences (Brown et al., 2003).

We expressed the CIF for each neuron as a function of movement direction, which corresponds to up, right, left, and down, and the neuron's spiking history in the preceding 150 ms. Instead of estimating the CIF continuously throughout the entire trial, we estimated it over 350 ms time windows around key epochs and at discrete time intervals, each 1 ms in duration. Specifically, we estimated the CIF over 350 ms windows centered at the gray array (GA) onset, TC onset, GC onset, and movement (MV) onset. We do not label each CIF with the corresponding epoch going forward for a simpler read and express the CIF as follows:

$$\lambda\,(t\,|\,H_t,\,\theta) = \lambda^S\,(t\,|\,\theta)\;\lambda^H\,(t\,|\,H_t,\,\theta) \qquad (3)$$

where $\lambda^S\,(t\,|\,\theta)$ describes the effect of the movement direction stimulus on the neural response and $\lambda^H\,(t\,|\,H_t,\,\theta)$ describes the effect of spiking history on the neural response. θ is a parameter vector to be estimated from data. The units of $\lambda^S\,(t\,|\,\theta)$ are spikes per second, and $\lambda^H\,(t\,|\,H_t,\,\theta)$ is dimensionless. The idea to express the CIF as a product of a stimulus component and a temporal or spike history component was first suggested by Kass and Ventura (2001). This idea is appealing, as it allows one to assess how much each component contributes to the spiking propensity of the neuron. If spiking history is not a factor associated with neural response, then $\lambda^H\,(t\,|\,H_t,\,\theta)$ will be very close to 1 for all times, and equation (1) reduces to an inhomogeneous Poisson process.

The model of the stimulus effect is as follows:

$$\lambda^S\,(t\,|\,\theta) = \alpha_d \mathrm{I}_d\,(t), \qquad (4)$$

where d = 1, 2, 3, 4 is the movement direction, $\mathrm{I}_d\,(t)$ = 1 if movement is in direction d, and 0 otherwise (indicator function).

The $\{\alpha_d\}$ parameters measure the effects of movement direction on the spiking propensity. Here, d = {1, 2, 3, 4} corresponds to {Up,Right,Down,Left}, respectively. For example, if α_1 is significantly larger than α_2, α_3, and α_4 during movement, then the probability that a neuron will spike is greater when the patient moves in the "up" direction, suggesting that the neuron itself may be tuned in the up direction.

Our model of spike history effect is as follows:

$$log(\lambda^H\,(t\,|\,H_t,\beta,\gamma)) = \sum_{j=1}^{10}\;\beta_j n\,(t-j : t-(j+1)) + \sum_{k=1}^{14}\;\gamma_k n\,(t-(10k+9):t-10k), \qquad (5)$$

where $n(a : b)$ is the number of spikes observed in the time interval $[a, b)$ during the epoch. The β_j parameters measure the effects of spiking history in the previous 10 ms, and therefore, can capture refractoriness and/or bursting on the spiking probability in the given epoch. For example, if $e^{\beta 1}$ is close to 0 for any given epoch, then for any given time t, if the neuron had a spike in the previous millisecond, then the probability that it will spike again is also close to 0 (due to the refractory period). Alternatively, if $e^{\beta 5}$ is significantly larger than 1, then for any time t, if the neuron had a spike 5 prior to t, then the probability that it will spike again is modulated up, suggesting bursting.

The γ_k parameters measure the effects of the spiking history in the previous 10–150 ms on spiking probability, which may be associated with not only the neuron's individual spiking activity, but also that of its local neural network. For example, if $e^{\gamma 4}$ is significantly larger than 1, then for any time t, if the neuron had ≥1 spikes between 40–50 prior to t, then the probability that it will spike again is modulated up, suggesting 20–25 Hz oscillations.

By combining equations (4) and (5), we see that the CIF may be written as follows:

$$log\,(\lambda(t\,|\,H_t,\beta,\gamma))=\alpha_d I_d+\sum_{j=1}^{10}\;\beta_j n\,(t-j : t-(j+1)) + \sum_{k=1}^{14}\;\gamma_k n\,(t-(10k+9) : t-10k), \qquad (6)$$

The model parameter vector $\theta = \{\alpha_d, \beta_j, \gamma_k\}$ contains 28 unknown parameters for each epoch and time

window modeled. We computed maximum-likelihood (ML) estimates for θ and 95% confidence intervals of θ for each neuron using glmfit.m in MATLAB.

Model fitting

Establishing the degree of agreement between a point-process model and observations of the spike train and associated experimental variables is a prerequisite for using the point-process analysis to make scientific inferences. We used Kolmogorov–Smirnov (KS) plots based on the time-rescaling theorem to assess model goodness-of-fit. The time-rescaling theorem is a well-known result in probability theory, which states that any point process with an integrable conditional intensity function may be transformed into a Poisson process with unit rate (Johnson and Kotz, 1970). A KS plot, which outlines the empirical cumulative distribution function of the transformed spike times versus the cumulative distribution function of a unit rate exponential, was used to visualize the goodness-of-fit for each model. The model is better if its corresponding KS plot lies near the 45° line. We computed 95% confidence bounds for the degree of agreement using the distribution of the KS statistic (Johnson and Kotz, 1970). If a model's KS plot was within the 95% confidence bounds, we included it in our analyses.

Making inferences from GLM parameters

As mentioned earlier, we built point-process models for STN neurons in seven PD patients and one healthy primate, which captured dynamics across four different epochs within a directed hand-movement task. (We summarize results for each species later.) For the PD data, 28 STN neuron models passed the KS test, and for the primate data, 35 models passed the KS test.

Recall from equation (2) that $\lambda(t \mid H_t)\Delta$ approximates the probability that the neuron will spike at time t given extrinsic and intrinsic dynamics up to time t, which is captured in H_t. By virtue of equation (6), we allowed the probability that each STN neuron would spike at some time t, to be modulated by movement direction, short-term history, and long-term history spiking dynamics. Figure 2 illustrates these three modulation factors on spiking activity for both PD and primate single-neuron models by plotting the optimal parameters and their corresponding 95% confidence bounds before and after MV onset. We made the following observations:

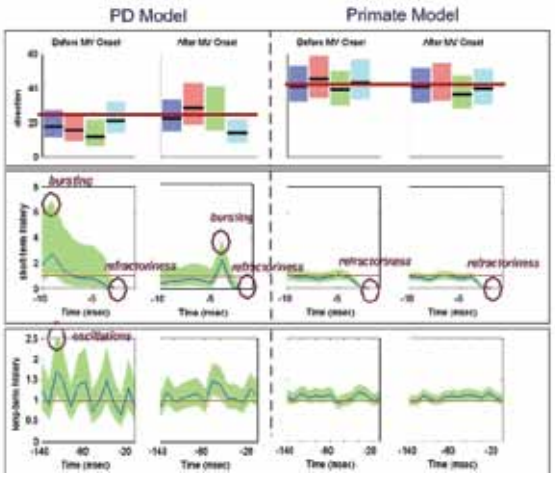

Figure 2. Optimal model parameters for an STN neuron during MV$^-$ and MV$^+$ periods of a (left) PD patient and (right) healthy primate. *Top row,* movement direction modulation. Optimal extrinsic factors $e^{\alpha d}$ for d = {1, 2, 3, 4} = {U,R,D,L} are plotted in black lines from left to right and corresponding 95% confidence intervals are shaded around each black line in a color. *Middle row,* short-term history modulation. Optimal short-term history factors $e^{\beta i}$ for i = 1, 2, ..., 10 are plotted in blue from right to left and the corresponding 95% confidence intervals are shaded in green. *Bottom row,* long-term history modulation. Optimal long-term history factors $e^{\gamma k}$ for k = 1, 2, ... , 14 are plotted in blue from right to left and corresponding 95% confidence intervals are shaded in green.

1. *Refractoriness:* As illustrated in the second row of Figure 2, both the PD and primate STN neuron exhibits refractory periods (Brodal, 1998), indicated by downmodulation by a factor of 10 or more due to a spike occurring 1 ms before a given time t. That is, if a spike occurs 1 ms before time t, then it is very unlikely that another spike will occur at time t ($e^{\beta i} \leq 1$ for all $e^{\beta i}$ within its 95% confidence band).

2. *Bursting:* As illustrated in the second row of Figure 2, the PD STN neuron spikes in rapid succession before and after MV onset, as indicated by one or more of the short- term history parameters ($e^{\beta i}$'s) corresponding to 2–10 ms in the past being larger than 1. That is, if a spike occurs 2–10 ms before time t, then it is more likely that another spike will occur at time t. Formally, a neuron bursts if its model parameters satisfy the following: for at least one i = 2, 3, ..., 10, $LB_i \geq 1$ and $UB_i \geq 1.5$, where $LB_i \leq e^{\beta i} \leq UB_i$. LB and UB are the 95% lower and upper confidence bounds, respectively.

NOTES

3. *10–30 Hz oscillations:* As illustrated in the third row of Figure 2, the PD STN neuron exhibits 10–30 Hz oscillatory firing before movement. That is, the probability that the PD STN neuron will spike at a given time t is modulated upward if a spike occurs 30–100 ms before time t. Formally, a neuron has 10–30 Hz oscillations if its model parameters satisfy the following for at least one $i = 2, 3, ..., 5$, $LB_i \geq 1$ and $UB_i \geq 1.5$, where $LB_i \leq e^{\gamma_i} \leq UB_i$.

4. *Directional tuning:* As illustrated in the first row of Figure 2, the PD STN neuron appears to exhibit more directional tuning after MV onset. That is, the PD neuron seems more likely to spike in one direction more than at least one other direction. To quantify directional tuning, we performed the following test for each neuron, each time relative to onset, and each epoch:

   - For each direction $d = \{U,R,D,L\}$, compute $p_{d^*d} = P_r(e^{\alpha_{d^*}} > e^{\alpha_d}) = P_r(\alpha_{d^*} > \alpha_d)$ for $d \neq d^*$. Define $p_{dd} = 0$. Use the Gaussian approximation for α_d, which is one of the asymptotic properties of ML estimates to compute p_{d^*d}.
   - If $\max_d =_{1,2,3,4} p_{d^*d} \geq 0.975$, then the neuron exhibits directional tuning.

In Sarma et al. (2010), we made the following observations across all neurons in both groups. Most neurons in both subject groups exhibit refractoriness. Bursting is prevalent across all epochs in neural activity of PD patients (on average, 39% of PD STN neurons burst). In contrast, neural activity in the healthy primate exhibits little bursting (14% on average) across all epochs. Oscillations of 10–30 Hz are prevalent in neural activity of PD patients across all epochs (on average, 36%) and significantly decrease relative to this baseline after movement. Beta oscillations have been observed experimentally in both parkinsonian primates and PD patients (Bergman et al., 1994; Raz et al., 2000; Bevan et al., 2002; Brown, 2003; Dostrovsky and Bergman, 2004; Montgomery, 2008), and attenuation of these oscillations postmovement has also been observed (Armirnovin et al., 2004; Williams et al., 2005). In contrast, an average of 12% of the primate neurons exhibit 10–30 Hz oscillations, which does not significantly modulate across the entire trial. Directional tuning is more prevalent in the healthy primate across the trial. In particular, directional tuning increases significantly above baseline right after the GA is shown in the primate case. This observation makes sense, as the primate knows and moves to one of the four possible directions shown. Tuning increases further in the primate neurons after the TC appears, as now the subject knows which direction to move when cued to do so. In contrast, directional tuning fails to increase significantly above baseline until right before MV onset in PD STN neurons. The lack of significant increase in directional tuning in PD STN neurons early in the trial may reflect the lack of a dynamic range in the STN neurons of PD patients, which may cause their slow and impaired movements.

Conclusion

We applied the point-process framework to the analysis of STN microelectrode recordings from PD patients and a healthy nonhuman primate, to understand the relative importance of movement and spiking history for neural responses. We used GLM representations of the point-process CIF to develop an efficient likelihood-based approach to model fitting, goodness-of-fit assessment, and inference. The point-process model parameters allowed us to identify pathological characteristics of the STN neurons in PD patients, including bursting, 10–30 Hz oscillations, and decreased directional tuning prior to movement. These characteristics, which differed from those of the non-PD STN neurons, had been previously described using traditional methods. However, such techniques can lead to erroneous inferences when spiking data contain significant temporal dependencies, as is the case for PD STN spiking activity. The point-process framework is therefore a useful paradigm for providing a succinct, quantitative characterization of the pathological behavior of STN spiking activity in PD patients.

Acknowledgment

This case report was originally published in the journal *IEEE Transactions on Bio-medical Engineering*. IEEE Trans Biomed Eng (2010) 57(6):1297–1305.

References

Armirnovin R, Williams ZM, Cosgrove GR, Eskandar EN (2004) Visually guided movements suppress subthalamic oscillations in Parkinson's disease patients. J Neurosci 24(50):11302–11306.

Bergman H, Wichman T, Karmon B, DeLong MR (1994) The primate subthalamic nucleus. II. Neuronal activity in the MPTP model of parkinsonism. J Neurophysiol 72:507–520.

Bevan MD, Magill PJ, Terman D, Bolam JP, Wilson CJ (2002) Move to the rhythm: Oscillations in the subthalamic nucleus-external globus pallidus network. Trends Neurosci 25:525–531.

Brown EN (2005) Theory of point processes for neural systems. In: Methods and models in Neurophysics, Chap 14 (Chow CC, Gutkin B, Hansel D, Meunier C, Dalibard J, eds), pp 691–726. Paris: Elsevier.

Brown EN, Barbieri R, Eden UT, and Frank LM (2003) Likelihood methods for neural data analysis. In: Computational neuroscience: a comprehensive approach, Chap 9 (Feng J, ed), pp 253–286. London: CRC.

Brown P (2003) Oscillatory nature of human basal ganglia activity: relationship to the pathophysiology of Parkinson's disease. Mov Disord 18:357–363.

Dostrovsky J, Bergman H (2004) Oscillatory activity in the basal ganglia: relationship to normal physiology and pathophysiology. Brain 127:721–722.

Montgomery E Jr (2008) Subthalamic nucleus neuronal activity in Parkinson's disease and epilepsy subjects. Parkinsonism Relat Disord. 14(2):120–125.

Raz A, Vaadia E, Bergman H (2000) Firing patterns and correlations of spontaneous discharge of pallidal neurons in the normal and the tremulous 1-methyl-4-phenyl-1,2,3,6-tetrahydropyridine vervet model of parkinsonism. J Neurosci 20(22):8559–8571.

Sarma SV, Cheng M, Williams Z, Hu R, Eskandar E, Brown EN (2010) Comparing healthy and parkinsonian neuronal activity in sub-thalamic nucleus using point process models. IEEE Trans Biomed Eng 57(6):1297–1305.

Truccollo W, Eden UT, Fellow MR, Donoghue JP, Brown EN (2005) A point process framework for relating neural spiking activity for spiking history, neural ensemble and extrinsic covariate effects. J Neurophys 93:1074–1089.

Williams ZM, Neimat JS, Cosgrove GR, Eskandar EN (2005) Timing and direction selectivity of subthalamic and pallidal neurons in patients with Parkinson disease. Exp Brain Res 162(4):407–416.